Data-Driven Digital Twins for Monitoring the Health and Performance of Converters

Yingpei Li
Dept. of ECE
University of Houston
Houston, United States
yli146@uh.edu

Bharat Bohara
Dept. of ECE
University of Houston
Houston, United states
bbohara@uh.edu

Harish Sarma Krishnamoorthy
Dept. of ECE
University of Houston
Houston, United States
hskrishn@central.uh.edu

Jeevanand Seshadrinath
Dept. of EE
Indian Institute of Technology Roorkee
Roorkee, India
jeevanand.seshadrinath@ee.iitr.ac.in

2024 IEEE International Communications Energy Conference (INTELEC) | 979-8-3503-7057-7/24/$31.00 ©2024 IEEE | DOI: 10.1109/INTELEC60315.2024.10679029

***Abstract*—This work introduces a machine learning approach for developing Digital Twins (DTs) for DC-DC converters, focusing on in-situ implementation in real-world operational conditions. A system based on a boost converter has been developed in MATLAB Simulink. To mirror real-world scenarios, commercial datasheets along with a range of input parameters, health degradation elements, temperature influence, and random noises have been considered. The study employs Multi-Layer Perceptron (MLP), Convolutional Neural Network (CNN), and Recurrent Neural Network (RNN) for predicting critical circuit responses of the boost converter, including inductor current, output voltage, and efficiency. Investigations show that MLP performs relatively poorly in the presence of noise. The CNN and RNN outperform the MLP under various noise levels, with the RNN exhibiting the best performance. This work advances DTs technology in power electronics, aiming to improve converter system optimization and enable predictive maintenance.**

***Index Terms*—Health Degradation, Temperature Influence, Noise Resilience, Multi-Layer Perceptron (MLP), Convolutional Neural Network (CNN), Recurrent Neural Network (RNN), Digital Twins (DTs), Predictive Maintenance**

I. Introduction

Digital Twin (DT) technology, emerging in the early 2000s, has become a cornerstone of Industry 4.0, significantly enhancing production efficiency, particularly in conjunction with the Internet of Things (IoT) [1]. By creating virtual replicas of physical entities, DTs enable real-time monitoring and optimization, facilitating predictive maintenance and reducing downtime. This integration is pivotal in modern industrial applications, where the synchronization of physical and digital realms can lead to significant improvements in operational efficiency and resiliency.

In power electronics, DTs are instrumental in merging hardware with computational models, offering a viable alternative to traditional simulation techniques [2]. Power converters that are crucial in energy management systems benefit immensely from DTs by being provided insights into their performance and health status. DTs that are lighter in memory use can significantly assist in monitoring and improving the health and performance of power converters by enabling in-situ implementation. This aspect is critical for converters, where real-time and rapid data processing is essential for maintaining stability and efficiency.

Modeling is the first step involved in the development of DTs. Conventional converter modeling methods, including circuit theory and state-space averaging, face challenges in providing a quick response while accurately simulating real-world scenarios [3]. However, for dynamic analysis of the circuit's performance as well as reliability, the evaluation must happen quickly. Hence, this work proposes a data-driven approach to develop a model for DTs for DC-DC converters, taking a system based on a boost converter in MATLAB Simulink as an example. This paper incorporates commercial device specifications, switching losses, component health degradation, temperature influence, and external noise, to closely emulate practical operational conditions. By integrating these factors, the system provides a realistic representation of the converter's performance, enhancing the reliability and robustness of the DTs. This approach ensures that the DTs for the boost converter can deliver valuable insights for system optimization and predictive maintenance.

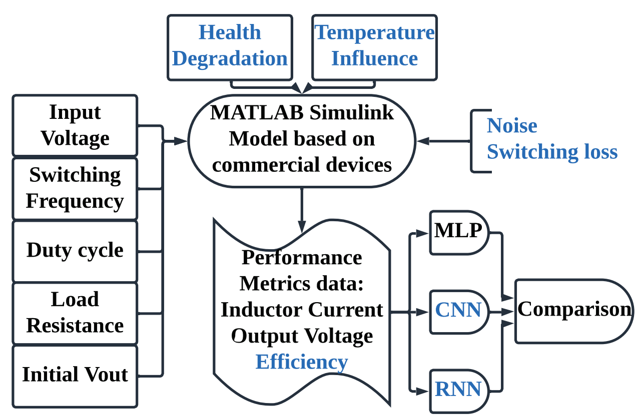

Fig. 1. Boost converter modeling flowchart.

As demonstrated in [2], the Multi-Layer Perceptron (MLP) has been effectively utilized for training models of power converters. This work also employs Convolutional Neural Network (CNN) and Recurrent Neural Network (RNN) models for DTs in performance prediction, with a specific focus on noisy environments. Both CNN and RNN architectures offer unique advantages. This diversified approach ensures that the model can adapt to different types of input data and operational conditions, providing a comprehensive solution for performance prediction.

This approach not only advances DTs in power electronics but also enhances system optimization and maintenance capabilities. By leveraging machine learning techniques, the model can continuously learn and adapt, improving its accuracy over time. This dynamic adaptability is essential for maintaining optimal performance in varying conditions, making it a valuable tool for predictive maintenance. Methodology and key contributions (highlighted in blue) of the study are outlined in Fig. 1, with subsequent sections discussing Simulink system construction (II), data-driven approaches comparison (III) and a conclusion with directions for future work (IV).

II. Structure and Design Details of the Boost Converter Simulink System

In this study, a boost converter's MATLAB Simulink model, detailed in Fig. 2, is considered, utilizing specifications of commercially available components to ensure practicality. The selection of these components is crucial as they directly impact the circuit responses of the converter.

The components chosen for the simulation include:

- **Diode:** CLH05(T6L,NKOD,Q) from Toshiba Semiconductor and Storage.
  - **Specifications:** Voltage rating: 200 V, Current rating: 5 A, Forward voltage drop: 0.85 V, Peak reverse current: 10^{-5} A, Reverse recovery time: 3.5×10^{-8} s [4].
- **MOSFET:** RCD050N20TL from ROHM.
  - **Specifications:** Voltage rating: 200 V, Current rating: 5 A, Drain-source on resistance: 0.47 Ω, Rise time: 1.5×10^{-8} s, Fall time: 1.1×10^{-8} s [5].
- **Inductor:** C-60U from Triad Magnetics.
  - **Specifications:** Current rating: 22.5 A, Inductance: 0.005 H, DC Resistance: 0.06 Ω [6].
- **Capacitor:** ALS70A822QC250-ND from KEMET.
  - **Specifications:** Voltage rating: 250 V, Capacitance: 0.0082 F, Equivalent Series Resistance: 0.041 Ω [7].

The specifications of these components impact switching loss, efficiency, voltage gain, and other circuit responses. Additionally, the Simulink system integrates switching losses, health degradation, temperature influence, and noise, simulating real-world conditions more accurately. By incorporating these factors, the simulation provides a comprehensive view of the boost converter's performance, accounting for practical challenges that may arise during actual operation.

A. Integration of Noise

The simulation's robustness is enhanced by incorporating stochastic elements, which are crucial for addressing uncertainties arising from manufacturing variances and environmental factors. These factors include electromagnetic interference and thermal fluctuations, both of which can significantly impact the performance of power converters in real-world applications. To accurately reflect these conditions, the system, as depicted in Fig. 2 ('Controlled Voltage Source' block), includes a configurable random white noise source. This noise source is designed to mimic various noise levels, thereby further aligning the simulation with practical scenarios.

The noise level in the simulation is represented by the signal-to-noise ratio (SNR) parameter. SNR is a critical metric in signal processing, quantifying the ratio of the power of a signal to the power of background noise. For Gaussian-distributed white noise, which is commonly used in simulations to represent random noise, the mean value is zero. In this context, the standard deviation of the noise is equal to the noise root mean square (RMS) value. This RMS value is instrumental in calculating the SNR, providing a standardized measure of noise level in the system [8].

B. Integration of Switching Loss

An accurate system of boost converters necessitates the integration of switching losses, especially when the system is based on commercial device datasheets. MATLAB Simulink's standard system typically omits these losses in MOSFETs and diodes, thus requiring a tailored system for incorporating them. Switching loss equations, sourced from Toshiba [9] and ROHM [10] for the specific diode and MOSFET used, facilitate the calculation of energy dissipation during switching. The diode's switching loss is represented as:

$$P_{sw} \approx \frac{1}{2} i_{rr} \times t_{rr} \times V_R \times f_{sw} \tag{1}$$

where i_{rr} is peak reverse current, t_{rr} is reverse recovery time, V_R is steady-state reverse voltage and f_{sw} is switching frequency. Similarly, the MOSFET's switching loss is given by:

$$P_{sw} = \frac{1}{2} V_{DS} \times I_D \times (t_r + t_f) \times f_{sw} \tag{2}$$

where V_{DS} denotes drain-to-source voltage in off-state, I_D is drain current in on-state, t_r is rise time, t_f is fall time and f_{sw} is switching frequency. (1) and (2) are integrated into the Simulink system via 'MATLAB Function' blocks, enhancing the simulation's precision and reflecting real-world operational conditions more accurately, as illustrated in Fig. 2 ('Efficiency' subsystem). This approach significantly enriches the simulation's fidelity, offering insights into the converter's efficiency and thermal performance, which are key in the development of high-fidelity DTs for power electronics.

C. Integration of Health Degradation

The reliability of power conversion systems is closely linked to the health status of individual components, which play a pivotal role in ensuring system longevity and performance stability. Among these components, capacitors, and MOSFETs are particularly critical due to their susceptibility to early degradation. The failure of these two components can lead to significant performance issues and system downtime, which underscores the importance of monitoring their health status closely [11].

Given the highest failure rates of these two components in static power converters, it is essential to utilize key degradation

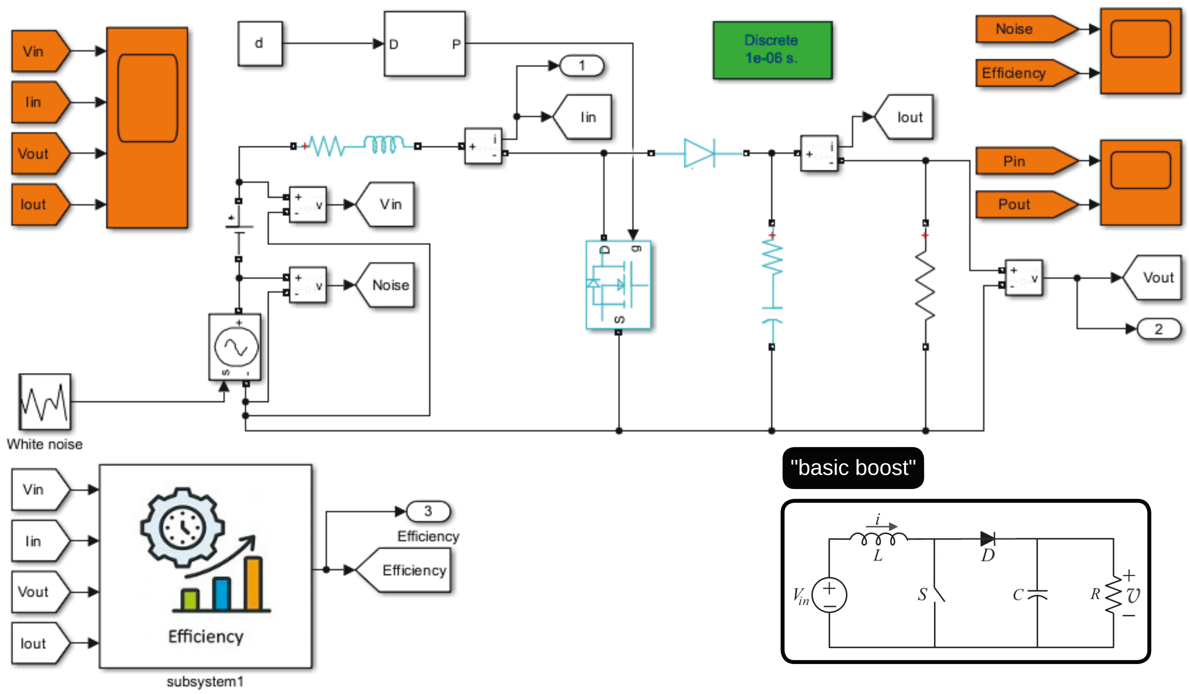

Fig. 2. MATLAB Simulink system of a boost converter.

indicators such as capacitance (C), equivalent series resistance (ESR), and drain-source on resistance (R_{dson}) to assess health degradation effectively. The degradation fault limits for electrolytic capacitors and MOSFETs are summarized in Table I [12]. These limits provide a benchmark for determining when a component has degraded to a point that it may no longer function effectively within the system. In the MATLAB Simulink system, the parameter 'useful health' is employed to represent the health level of the devices.

At a given temperature (say, room temperature), 100% 'useful health' corresponds to the nominal value of the health indicator, indicating that the component is in optimal condition. Conversely, 0% 'useful health' corresponds to a 'close-to-a-fault' value, signifying that the component has reached a critical level of degradation and may fail in the near future or may not meet certain performance criteria. By incorporating these degradation indicators and fault limits into the simulation, the model can more accurately reflect the real-world performance and longevity of the power converter.

TABLE I
DEGRADATION FAULT LIMITS (BASED ON AMBIENT TEMPERATURE MEASUREMENTS)

Degradation indicator	Limit
ESR	Increase to twice the nominal value
C	Decrease to 80% of the nominal value
R_{dson}	Increase to 125% of the nominal value

D. Integration of Temperature Influence

The performance of components in the boost converter is significantly influenced by temperature variations. For the diode, the forward voltage drop (V_f) serves as a temperature influence indicator. The relationship between temperature and V_f can be referenced from the datasheet [4]. For the MOSFET, the drain-source on resistance (R_{dson}) is selected as the temperature influence indicator, with its relationship to temperature detailed in the datasheet [5].

For capacitors, both equivalent series resistance (ESR) and capacitance (C) are chosen as indicators of temperature influence. The relationship between temperature and these indicators can be obtained from [13] and through reasonable assumptions. For inductors, the direct current resistance (DCR) is the indicator, with changes due to temperature represented by the temperature coefficient of copper.

All relevant information is summarized in Table II.

TABLE II
TEMPERATURE INFLUENCE ON INDICATORS

Indicator	Change per $^{\circ}C$
V_f	Decrease by 0.24%
R_{dson}	Increase by 0.37857%
ESR	Decrease by 1%
C	Increase by 0.1%
DCR	Increase by 0.393%

III. Converter Performance Metrics Modeling with Data-Driven Approaches

This study focuses on modeling the dynamic behavior of a boost converter using data-driven methodologies. The aim is to simulate responses such as output voltage, inductor current, and efficiency, based on various converter parameters including input voltage, frequency, duty cycle, load resistance, initial output voltage, temperature, and useful health. The specific ranges for these parameters are detailed in Table III.

Additionally, the system incorporates varying levels of noise, aiming to simulate realistic operating conditions.

TABLE III
RANGE OF PARAMETERS FOR BOOST CONVERTER MODELING

Parameter	Range
Vin (V)	15 – 45
Duty cycle (%)	40 – 60
Frequency (kHz)	10 – 30
Load Resistance (Ω)	60 – 100
Initial Vout (V)	0 – 10
Temperature ($°C$)	-20 – 80
Useful health (%)	0 – 100

A. Data Collection and Processing

High-quality simulation data, crucial for model accuracy, was gathered from MATLAB simulations. This data spanned key parameters (input voltage, duty cycle, switching frequency, load resistance, initial output voltage, temperature, and useful health) and circuit responses (temporal responses of the inductor current, output voltage, and efficiency). The original high-resolution dataset of 800,000 data points for each circuit response was recorded (resolution of 1 µs over a span of 0.8 s). Due to the risk of overfitting with high-resolution data, a thorough pre-processing regimen involving downsampling and normalization was carried out to facilitate effective neural network training [2].

B. Brief Introduction to Various Data Driven Techniques Adopted

For the data obtained from the simulations, CNN and RNN were selected due to their unique characteristics and strengths compared to MLP, with the potential to improve upon the results. The MLP is a class of feedforward artificial neural networks that consists of multiple layers of nodes, with each layer fully connected to the next one. It is particularly effective for general-purpose pattern recognition problems and has been extensively used due to its simplicity and effectiveness in approximating continuous functions [14].

The CNN is designed to automatically and adaptively learn spatial hierarchies of features from input data. Additionally, CNN has shown robustness in environments with noise variability, as their deep architectures can filter out noise more effectively than MLP, enhancing prediction accuracy under noisy conditions [15].

The standard RNN (SimpleRNN) architecture is employed for training, characterized by its straightforward recurrence mechanism, distinguishing it from other RNN extensions. RNN are particularly well-suited for sequential data due to their connections that form directed cycles, allowing them to maintain a memory of previous inputs. This makes RNN particularly powerful for time-series prediction and data with temporal dependencies [16]. Given the dynamic nature of the boost converter's operation, RNN provides a robust framework for capturing temporal correlations. Compared to CNN, RNN are not only effective in environments with noise but are also more appropriate for tasks involving sequential data, such as predicting the behavior of the boost converter over time. This ability to handle time-dependent data makes RNN highly suitable for the given application.

Figure 3 presents the architectures of MLP, CNN, and RNN, showcasing their structural differences in this study.

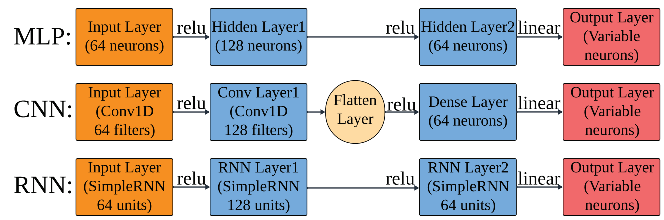

Fig. 3. Structures of MLP, CNN and RNN.

C. Comparison of MLP, CNN, and RNN Under Variable Noise Conditions

Initially, the performance of the neural networks was evaluated in the absence of noise to establish a baseline. Figure 4 presents the training and validation results for the Multi-Layer Perceptron (MLP). Figure 5 shows the results for the Convolutional Neural Network (CNN). Figure 6 illustrates the results for the Recurrent Neural Network (RNN). Part (a) of these figures illustrates the progression of model training, highlighting convergence in minimizing the cost function. Additionally, the training duration is displayed, indicating that the training times for all three models are comparable. Part (b) shows performance on regression plots. Parts (c), (d), and (e) display the validation results with specific parameter settings – [*Vin* $= 35V$; *Duty cycle* $= 40\%$; *Frequency* $= 30kHz$, *Load resistance* $= 73.3\Omega$; *Initial Vout* $= 10V$; *Temperature* $= 80°C$; *Useful health* $= 100\%$], depicting the simulated and predicted inductor current, output voltage, and efficiency. The inductor current and output voltage are shown in waveforms. The mean of the final 100 efficiency data points is used to determine the simulated and predicted efficiency.

Extensive simulations were then conducted to evaluate the performance of MLP, CNN, and RNN under varying levels of noise. The results, presented in Table IV, highlight the distinct features and advantages of each neural network model.

TABLE IV
R^2 VALUES FOR VARIOUS MODELS UNDER DIFFERENT NOISE LEVELS

Noise level/SNR (dB)	MLP	CNN	RNN
∞ (without noise)	0.97926	0.98059	0.98531
40	0.97940	0.98078	0.98643
35	0.97787	0.98236	0.98571
30	0.97883	0.98289	0.98402
25	0.97724	0.98112	0.98640
20	0.97564	0.98195	0.98482

The results demonstrate that while MLP, CNN, and RNN have similar training duration and high performance, the RNN outperforms both CNN and MLP. The MLP, known for its simplicity and effectiveness in general-purpose pattern recognition, showed a decline in performance with increased noise. In contrast, the CNN maintained stable R^2 values,

(a) (b)

(c) (d)

MLP without noise: Simulated and Predicted efficiency

Simulated Efficiency	Predicted Efficiency
0.9758	0.9010

(e)

Fig. 4. Training and validation results of MLP for data without noise: (a) Model loss over epochs and training duration (b) R^2 value (c) Simulated and predicted inductor current (d) Simulated and predicted output voltage (e) Simulated and predicted efficiency.

(a) (b)

(c) (d)

CNN without noise: Simulated and Predicted efficiency

Simulated Efficiency	Predicted Efficiency
0.9758	0.9589

(e)

Fig. 5. Training and validation results of CNN for data without noise: (a) Model loss over epochs and training duration (b) R^2 value (c) Simulated and predicted inductor current (d) Simulated and predicted output voltage (e) Simulated and predicted efficiency.

demonstrating its enhanced noise immunity and suitability for modeling power converters in noisy environments. The RNN slightly outperformed the CNN across various noise levels, exhibiting higher R^2 values and stable performance in noisy conditions. This can be attributed to the RNN's ability to capture temporal correlations and maintain the memory of previous inputs, making it particularly effective for time-series prediction and data with temporal dependencies.

Additionally, variants and extensions of RNN such as Gated Recurrent Units (GRU), Long Short-Term Memory (LSTM), and Bidirectional Long Short-Term Memory (BiLSTM) were also explored. Hybrid neural network architectures like CNN-LSTM and CNN-BiLSTM were tested as well. Despite the increased complexity of these models, their performance did not surpass that of the standard CNN and RNN models. Consequently, these more complex models were not included in the final results presented in this study.

D. Efficiency Prediction with RNN

Based on previous results, the RNN demonstrated superior performance in predicting converter efficiency. A trained RNN model for data without noise is utilized to predict efficiency under various conditions. For efficiency analysis, a set of fixed inputs is assumed: [*Duty cycle* $= 50\%$; *Frequency* $= 20kHz$; *Initial Vout* $= 5V$; *Temperature* $= 80°C$; *Useful health* $= 100\%$]. The *Load resistance* is varied in a range for each *Vin*.

Figure 7 presents the simulated and predicted efficiency against the load power at different *Vin* values. For each *Vin*, the varying effective *load resistance* results in differing load power and correspondingly, efficiency. The results indicate that the efficiency prediction accuracy is satisfactory, demonstrating that the RNN performs well under these conditions.

IV. Conclusion and Future Work

This work introduces a data-driven approach for developing digital twins (DTs) for power converters using MATLAB Simulink simulations. Critical factors such as switching losses, component health degradation, temperature influence, and noise interference are incorporated. The study employs CNN, RNN, and MLP models to predict critical responses, highlighting the performance of each model under various noise conditions. RNN perform best in handling temporal dependencies and maintaining stability in noisy environments, while CNN provides enhanced noise immunity. MLP, although effective for general-purpose pattern recognition, showed a decline in performance with increased noise.

These advancements can contribute to the development of DTs in power electronics, enabling improved system optimiza-

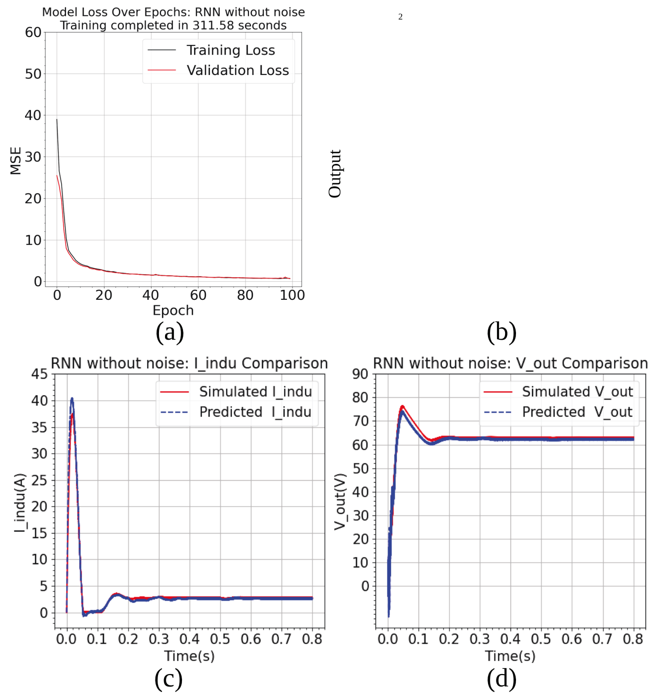

RNN without noise: Simulated and Predicted efficiency

Simulated Efficiency	Predicted Efficiency
0.9758	0.9728

(e)

Fig. 6. Training and validation results of RNN for data without noise: (a) Model loss over epochs and training duration (b) R^2 value (c) Simulated and predicted inductor current (d) Simulated and predicted output voltage (e) Simulated and predicted efficiency.

Fig. 7. Efficiency against Load Power at different input voltages.

tion and predictive maintenance. The proposed approaches are expected to enhance in-situ DTs (by making them lighter in memory use), automated design, and software-defined networks, providing efficient modeling solutions. The compatibility of these models with GPUs or FPGAs aligns with advancements in edge computing for power converters, presenting promising avenues for future research and implementation.

V. Acknowledgement

This work is supported by the National Science Foundation (NSF) under Grant No. 2239966. This project involved collaboration between the University of Houston and the Indian Institute of Technology, Roorkee, partially supported by SERB, DST SIRE Scheme, Govt of India.

References

[1] M. W. Grieves, ”Virtually Intelligent Product Systems: Digital and Physical Twins,” Complex Systems Engineering: Theory and Practice, 2019. [Online]. Available: https://api.semanticscholar.org/CorpusID:202478997
[2] H. S. Krishnamoorthy and T. Narayanan Aayer, ”Machine Learning based Modeling of Power Electronic Converters,” in *2019 IEEE Energy Conversion Congress and Exposition (ECCE)*, 2019, pp. 666-672. doi: 10.1109/ECCE.2019.8912608
[3] Q. Shang, F. Xiao, Y. Fan, W. Kang, H. Qin, and R. Wang, ”Effinformer: A Deep-Learning-Based Data-Driven Modeling of DC–DC Bidirectional Converters,” *IEEE Transactions on Instrumentation and Measurement*, vol. 72, pp. 1-13, 2023. doi: 10.1109/TIM.2023.3318701
[4] Toshiba Corporation, ”TOSHIBA High-Efficiency Rectifier - Silicon Epitaxial Type CLH05,” CLH05(T6L,NKOD,Q) datasheet, Nov. 2013.
[5] Rohm Semiconductor, ”10V Drive Nch MOSFET RCD050N20,” RCD050N20TL datasheet, Sept. 2011.
[6] Triad Magnetics, ”Triad Magnetics Inductors C-60U,” C-60U datasheet, Dec. 2013.
[7] KEMET Corporation, ”Screw Terminal Aluminum Electrolytic Capacitors ALS70/71, High CV, +85°C,” ALS70A822QC250-ND datasheet.
[8] S. Arar. (2019, Nov. 20). Noise in Electronics Engineering: Distribution, Noise RMS and Peak-to-Peak Value, and Power Spectral Density [Online]. Available: https://www.allaboutcircuits.com/technical-articles/noise-in-electronics-engineering-distribution-noise-rms-peak-to-peak-value-PSD/
[9] Toshiba Corporation, ”Basics of Diodes (Power Losses and Thermal Design),” Application Note, Aug. 2021.
[10] Rohm Semiconductor, ”Calculation of Power Loss (Synchronous),” Application Note, Oct. 2016.
[11] A. Rahnama Sadat and H. Sarma Krishnamoorthy, ”Measure Theory-based Approach for Remaining Useful Lifetime Prediction in Power Converters,” in *2020 IEEE Energy Conversion Congress and Exposition (ECCE)*, 2020, pp. 2541-2547. doi: 10.1109/ECCE44975.2020.9235635
[12] R. A. Plazas Rosas, É. Mejía, and M. Orozco-Gutiérrez, ”Degradation indicators for power electronic converters,” Revista Tecnología en Marcha, vol. 36, pp. 23-28, June 2023. doi: 10.18845/tm.v36i6.6751
[13] A. Chidley. (2017, Mar. 01). Understanding ESR in electrolytic capacitors [Online]. Available: https://my.avnet.com/abacus/resources/article/understanding-esr-in-electrolytic-capacitors/
[14] D. E. Rumelhart, G. E. Hinton, and R. J. Williams, ”Learning representations by back-propagating errors,” *Nature*, vol. 323, pp. 533-536, 1986. [Online]. Available: https://api.semanticscholar.org/CorpusID:205001834
[15] A. Krizhevsky, I. Sutskever, and G. E. Hinton, ”ImageNet classification with deep convolutional neural networks,” *Communications of the ACM*, vol. 60, pp. 84-90, 2012. [Online]. Available: https://api.semanticscholar.org/CorpusID:195908774
[16] A. Graves, ”Supervised Sequence Labelling with Recurrent Neural Networks,” in *Studies in Computational Intelligence*, 2012. [Online]. Available: https://api.semanticscholar.org/CorpusID:2118350